Journal of Power Sources 242 (2013) 775–783

Contents lists available at SciVerse ScienceDirect

Journal of Power Sources

journal homepage: www.elsevier.com/locate/jpowsour

Effect of binder burnout on the sealing performance of glass ceramics for solid oxide fuel cells

Tugrul Y. Ertugrul [a,*], Selahattin Celik [a,b], Mahmut D. Mat [a]

[a] HYTEM, Nigde University, Mechanical Engineering Department, Nigde University Campus, 51245 Nigde, Turkey
[b] Gazi University, Mechanical Engineering Department, 06570 Ankara, Turkey

HIGHLIGHTS

- Effects of binder burnout on sealing quality of solid oxide fuel cells.
- Effect of heating rate, solid loading, sweep gas type and their flow rate and pressure on the cells is considered.
- The heating rate and sweep gas mass flow rate are found to be critically important on the quality of sealing.
- The burnout and sealing quality are analyzed through leakage rate and macrostructure.

ARTICLE INFO

Article history:
Received 16 January 2013
Received in revised form
15 May 2013
Accepted 23 May 2013
Available online 5 June 2013

Keywords:
Solid oxide fuel cell
Glass–Ceramics
Binder Burnout
Sealing behavior

ABSTRACT

The glass ceramics composite sealants are among few materials suitable for the solid oxide fuel cells (SOFC) due to their high operating temperatures (600 °C–850 °C). The glass ceramics chemically bond to both the metallic interconnector and the ceramic electrolyte and provide a gas tight connection. A careful and several stages manufacturing procedure is required to obtain a gas tight sealing. In this study, effects of binder burnout process on the sealing performance are investigated employing commercially available glass ceramic powders. The glass ceramic laminates are produced by mixing glass ceramic powders with the organic binders and employing a tape casting method. The laminates are sandwiched between the metallic interconnectors of an SOFC cell. The burnout and subsequent sealing quality are analyzed by measuring leakage rate and final macrostructure of sealing region. The effects of heating rate, dead weight load, solid loading, carrier gas and their flow rates are investigated. It is found that sealing quality is affected from all investigated parameters. While a slower heating rate is required for a better burnout, the mass flow rate of sweep gas must be adequate for removal of the burned gas. The leakage rate is reduced to 0.1 ml min^{-1} with 2 °C min^{-1} + 1 °C min^{-1} heating rate, 86.25% solid loading, 200 N dead weight load and 500 ml min^{-1} sweep gas flow rate.

1. Introduction

Solid oxide fuel cells (SOFC) are a promising technology for electrical energy production through electrochemical conversion. They have been studied extensively in recent years because of their high energy conversion efficiency, low carbon dioxide emission, fuel flexibility, high power density per unit volume and possibility of co-generation. However, there are several technological problems which must be solved for a market acceptance and extending their application areas. As SOFC's operate at high temperatures (700 °C–850 °C) sealing is currently one of the most important issues especially for a planar type SOFC. Leakage during the fuel cell operation may cause serious safety problems, decrease in performance and even catastrophic failure of the SOFC cell or stack.

Glass ceramics have been regarded as a candidate material for SOFC sealing. In recent years, numerous studies have been carried out to develop appropriate glass ceramics for a leak free and durable sealing [1–8]. Several new glass–ceramic compositions have already met some important requirements such as thermal and chemical stability under dual environmental conditions (oxidizing and reducing), excellent sealing properties at elevated temperatures (600 °C–850 °C), sufficient electrical stability and adequate thermal expansion (CTE) match with the electrolyte and the metallic interconnect materials [1–8].

The glass ceramic sealants predominantly exhibit ceramic properties and are usually fabricated employing ceramic production

* Corresponding author. Tel.: +90 388 225 27 97; fax: +90 388 225 01 12.
E-mail address: tyertugrul@nigde.edu.tr (T.Y. Ertugrul).

0378-7753/$ – see front matter © 2013 Elsevier B.V. All rights reserved.
http://dx.doi.org/10.1016/j.jpowsour.2013.05.106

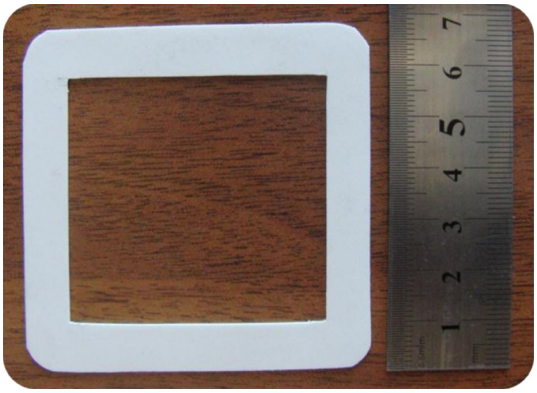

Fig. 1. The tape casted glass ceramic sheets.

methods (i.e., mixing, casting, binder burnout and sintering). The mixing step so-called "solid loading" involves mixing ceramic powders with organic additives. A variety of additives such as binder, plasticizer, dispersant and solvent are used to improve workability and the mechanical strength of green body of glass ceramic sealants [9–13]. In the casting step, different techniques (extrusion, slip casting, injection molding, tape casting) can be used depending on the sealing applications. The tape casting is one of the most convenient casting methods for the glass ceramics as it produces ceramic laminates with desired geometry and very tight dimensional accuracy [9–13]. The binder burnout and the sintering are thermal steps which critically affect the quality of the final product.

The binder burnout which is the most likely stages to form defect (cracks, blister, distortion, and bubbles development) is the key process in the production of a ceramic. The decomposition of organic additives may cause a pressure buildup inside the green body. If any uncontrolled burnout occurs inside the body, large internal pressure can be generated, which may result in defects and cracks in the final product. Many ceramic processing for a number of final critical properties involves binder burnout and sintering steps such as high dimensional tolerances in electronics applications [14], high precise surface quality (zirconia 3Y-TZP) for ceramic micro components [15], mechanical strength (Titanium alloy–hydroxyapatite, Ti-6Al-4V/HA) for biomedical application [16], etc. Safe removal of the organic component from green body is essential for higher quality of final products.

The binder burnout is a complex process involving the polymer decomposition, transport and diffusion of decomposed products, and removal of them. A number of parameters; ceramic body compact size, shrinkage rate, heating rate, sweeping gas type and its flow rates, organic polymer type and its volume fraction may critically affect burnout process [17–22]. Numerous experimental and theoretical studies are available in the literature on the determination of the burnout kinetics, estimation of temperature and stress distribution effects of processing parameters on the burnout and subsequent powder distribution in the ceramic body [23–26]. However, these studies mainly involve injection molded ceramics, only few studies consider the ceramic laminates [17–19]. To the best knowledge of authors no study considers effects of binder burnout process on sealing quality of the glass ceramic composites. The burnout and sintering of the glass ceramics are further complicated as the glass ceramics laminates are packed between a metallic interconnector and a ceramic electrolyte during the burnout and sintering processes.

In this study, effects of the binder burnout on the glass ceramic sealing quality are investigated. Effects of temperature (different heating rates), pressure (dead weight load), solid loading (glass powder/binder ratios), carrier gas type (nitrogen and air) and their flow rates are experimentally investigated, and optimum parameters for a better sealing are determined.

2. Experimental

2.1. Glass seal preparation

Commercial glass ceramic powders (Viox-V1649, Seattle, USA) were mixed with an organic dispersant (fish oil, Sigma–Aldrich, Munich, Germany) and solvent (ethyl alcohol, Sigma–Aldrich). After ball milling around 12 h, certain amount of plasticizer (polyethylene glycol, Sigma–Aldrich) and binder (Butvar, Sigma–Aldrich) were added. The composition of glass ceramic powder is mainly B_2O_3, SrO, La_2O_3 [27]. The mixture was ball milled again for another 12 h. Then the slurry was tape casted with a blade gap of

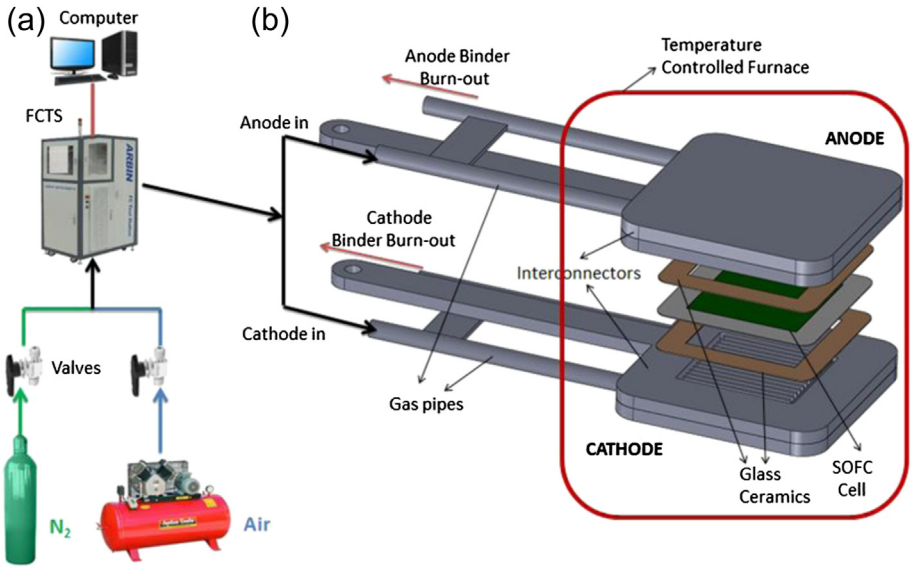

Fig. 2. Schematics of SOFC test setup (a) and test fixture (b).

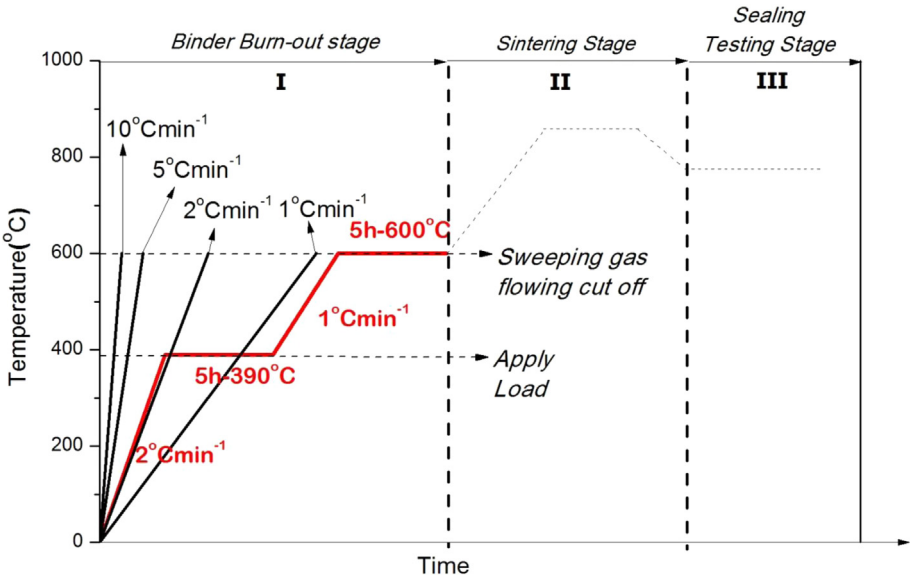

Fig. 3. Heating schedule.

200 μm (Keko Equipment Ltd., CAM-L252TB, Zuzemberk, Slovenia). Sufficient amount of glass tapes of 1 mm thickness were stacked together and laminated under isostatic pressure (40 MPa) for 4 min. The laminates were then cut into a square window frame (70 mm × 70 mm and 60 mm × 60 mm) using a laser cutter (Versa Laser, VSL2.3, Australia). The ready to use glass–ceramic laminates are shown in Fig. 1. The corners of the laminates were tapered to fit into the SOFC test cell by a laser cutter.

2.2. Experimental setup and testing

The experimental setup employed for SOFC and testing is shown in Fig. 2. The setup involves a test fixture, a temperature controlled furnace, an SOFC test station (Arbin Instruments, FCTS, Texas, USA), a computer, nitrogen and air gas tanks. The furnace has a push rod which can apply a load ranging from 0 to 600 N. The test fixture consists of two metallic interconnectors which are made of a special high corrosion resistant alloy, Crofer22APU (Thyssen Krupp, Germany), two glass ceramic sealant (for anode and cathode sides) and in house fabricated electrolyte-supported SOFC cell with an active area of 16 cm^2 (4 cm × 4 cm). Scandia-doped zirconia (ScSZ), nickel oxide (NiO) and *lanthanum strontium manganite* (LSM) are employed as electrolyte, anode and cathode respectively in the cell. The fabrication procedure of the SOFC cells is given in Refs. [28–30]. All components are stacked between two interconnectors. The details of the short stack configuration are shown in Fig. 2b.

Two different gases (N_2 and air) were used for sweeping burned organics (Fig. 2a). While N_2 was supplied from a commercial nitrogen tank, an air compressor equipped with a 250 l storage tank and oil and moisture filters were used to supply air. Sweeping gases were fed into the short stack from the anode and cathode manifolds. The interconnector gas pipes were used to supply fresh gas and remove burned ingredients. During the binder burnout stage (stage-I) a range of flow rates between 100 ml min^{-1} and 1000 ml min^{-1} were tested. After 600 °C where no organics left in the sealant, the sweeping gas was cut off.

Heating schedule applied during the burnout and sealing process is shown in Fig. 3. The heat treatment involves three stages; binder burnout (stage-I), sintering (stage-II) and testing (stage-III). In this paper, we are focused on the binder burnout stage (room temperature to 600 °C) and final leakage testing-stages. The glass ceramic samples (produced using the same procedure and have identical dimension) were tested at various heating rates. The binder burnout (up to 600 °C) was achieved at a four-stage based on thermogravimetric analysis (TGA) and manual of binder producer. The temperature linearly increased from room temperature to the first dwelling period (390 °C) and increased to 600 °C (the second dwelling period). A range of ramp rates and dwelling periods on quality of the sealing were investigated. The cases considered are summarized in Table 1.

The furnace has a push rod pressing capability which can apply a range of load on the short stack. From the beginning of the experiment, a dead weight was applied on the short stack from room temperature to 390 °C just to keep the stack together and allow the burnout gas can leave out of the stack easily. The effects of applied load (from 0 to 400 N) were investigated after 390 °C.

Fig. 4 shows leakage and sealing quality test system employed. After binder burnout and sintering stages all glass ceramic sealing were tested for gas leakage (stage-III). Two precise mass flow meters (Alicat Scientific Incorporated, Tucson, USA) with accuracy of 0.1 ml min^{-1} (sccm) were used to measure the leakage rate with N_2 inert gas. The idea of the sealing test system is based on measuring

Table 1
Effect of heating rates on leakage rates and observations (No-load, No sweep gas, and 80 (%wt) solid loading).

Exp.	Heating rates	Sealing qualities	Leakage rates (ml min^{-1})
1	10 °C min^{-1}	Catastrophic carbon deposition	**46.3**
2	5 °C min^{-1}	Binder burnout holes are joining together and forms channel (channel type joining)	**42.1**
3	2 °C min^{-1}	Binder burnout holes are joining together and generate channel but smaller (channel type joining)	**19.3**
4	1 °C min^{-1}	Binder burnout holes are joining together and forms islands	**15.8**
5	2 °C min^{-1} + 1 °C min^{-1}	Smaller islands formed	**11.4**

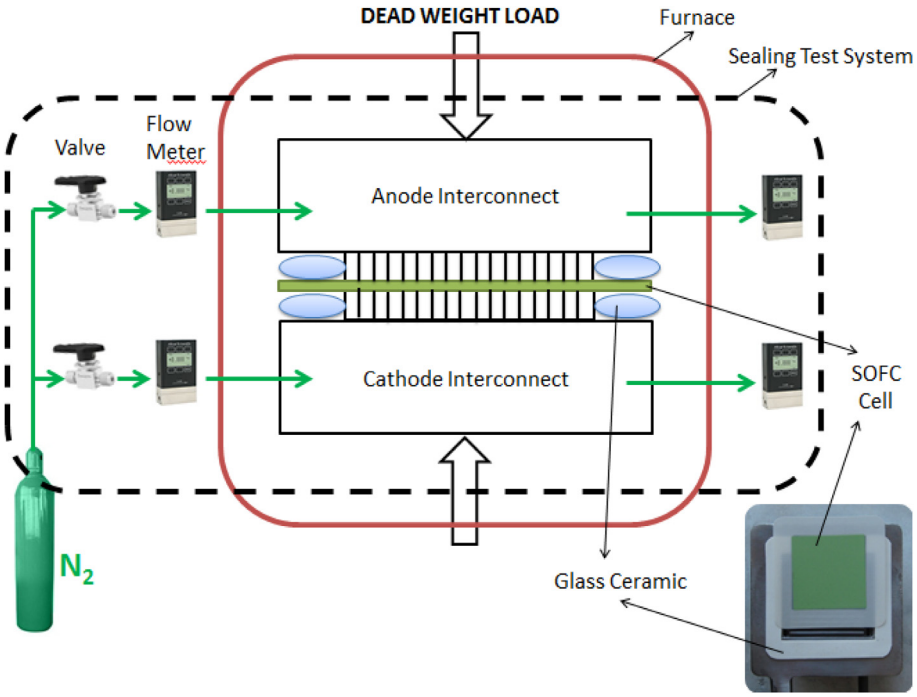

Fig. 4. Leakage test setup.

flow rate difference between the inlet and outlet. For all sealing tests, approximately 100 ml min^{-1} N_2 inert gas was supplied to the short stack. The mass flow rates of N_2 inlet and outlet were measured at the same time. The difference of mass flow rates shows leakage rates of the glass ceramic samples. The sealing tests were applied for both anode and cathode sides. The leakage tests were performed at 800 °C which is the operating temperature of SOFC stack.

3. Results and discussion

3.1. Effects of heating rate

Organics used in glass–ceramic laminate preparation process involve long chained polymers which produce mainly carbon dioxide during the burning. The produced gases must be removed carefully to achieve a better sealing. Accumulation of such gases in the sealing region may damage the integrity of the sealing in many ways leading a local pressure buildup and eventually break up of porous network forming large exhaust routes which prevents sintering the glass ceramic particles. The burned gas can escape only through a porous network which porosity depends on the solid loading, powder morphology and amount of organic burned. Effects of several heating rate on the sealing quality are investigated from 1 °C min^{-1} to 10 °C min^{-1}. An effect of the heating rate on the joining structure is shown in Fig. 5. 10 °C min^{-1} heating rate (Fig. 5a) a catastrophic carbon deposition is clearly visible which does not allow the glass–ceramic powders join together and resulting an unacceptable sealing. The carbon deposition and subsequent unsuccessful sealing are considered to be a result of excessive bond breaking, gas production and inadequate air feeding to the sealing region to remove all burned gas. The measured leakage rates depending on the heating rate are summarized in Table 1. It is seen that higher heating rates produces high leakages. A better sealing is obtained at lower heating rates. At 5 °C min^{-1} (Fig. 5b) the glass ceramics powders are joined at more locations and provide a better sealing. However the burned gas forms large paths to leave, resulting in a poor sealing performance. The large distances between particles prevent joining and sintering of the particles. The large exhaust paths are replaced by closed islands, (Fig. 5c and d) and smaller islands are formed at lower heating rates. The leakage rates decrease to 46.3 ml min^{-1}–15.8 ml min^{-1} by reducing heating rate from 10 °C min^{-1} to 1 °C min^{-1}. A further optimization is performed by applying a two-stage heating programs. Since decomposition of the binders is very low, a 2 °C min^{-1} heating rate is applied before 390 °C and 1 °C min^{-1} heating rate is kept at higher temperatures. This two-step heating program both speeds up the process and improves the sealing and reduces the leakage rate to 11.4 ml min^{-1}. However results show that even two stages heating cannot provide an acceptable sealing. It means that the heating rate is not only parameter for a leak-free sealing. Therefore, other effects are continued to be optimized.

3.2. Effects of solid loading

Binders, plasticizers and dispersants are added to glass–ceramics to obtain workable laminates through the tape casting method. The tape casting method is chosen since it produces glass–ceramic laminates with desired geometry for the planar SOFC stacks with very tight dimensional accuracy. The solid loading is defined as the ratio of the solid to total organic and solid in the tape. The effects of solid loading are investigated by reducing binder and plasticizer. The weight ratios of both organics are reduced 20–13%. It is very difficult to obtain an appropriate tape with a very low organic ratio then experiments are terminated after 13%. An effect of the organic ratio on the structure of the sealing is shown in Fig. 6. The heating rate is kept constant at optimized rate (2 °C min^{-1} + 1 °C min^{-1}) at all experiments. It is seen that the size of closed pores is clearly smaller with lower organics however, the pores still cannot be totally eliminated by just reducing the organic ratio. The solid loadings and corresponding tape quality, sealing quality and measured leakage rate summarized are in Table 2. The leakage with minimal organic

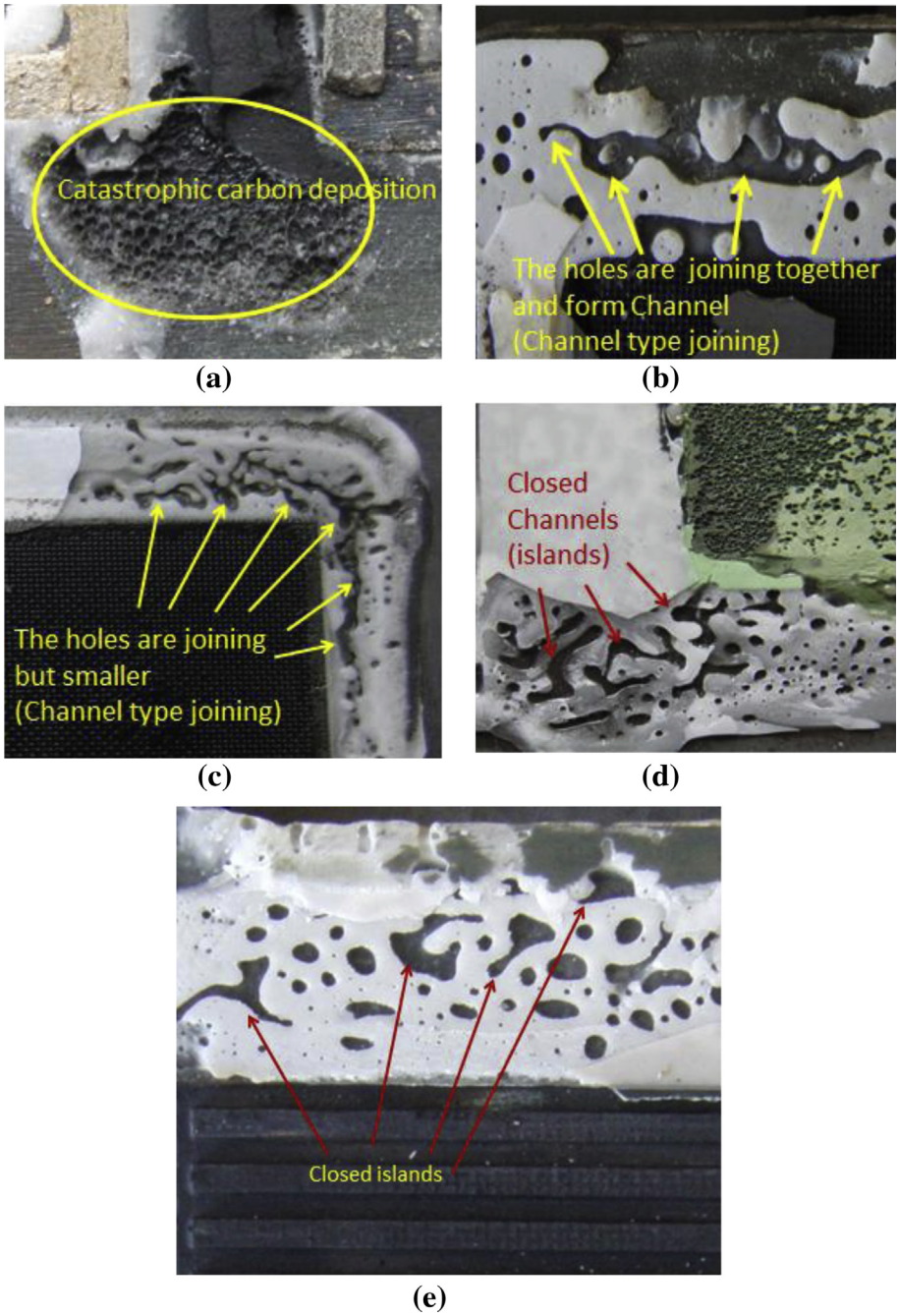

Fig. 5. The macrostructure of sealing after experiments (No-load, No sweep gas, and 80 (%wt) solid loading) (a) 10 °C min^{-1}, (b) 5 °C min^{-1}, (c) 2 °C min^{-1}, (d) 1 °C min^{-1}, (e) Desired heating rate (2 °C min^{-1} + 1 °C min^{-1}).

ratio also shows that some of the pores are still not connected allowing some of the gases to leave the gas chamber.

3.3. Sweep gas effect

The burned gas must be carefully removed from the sealing area to protect the ceramic structure and to prevent pressure built up. Therefore, the sweep gas and its flow rate have a great influence on quality of the sealing. The effects of nitrogen and air and flow rates ranging from 100 ml min^{-1} to 1000 ml min^{-1} are investigated. Nitrogen is chosen to prevent the metallic interconnector surface (at cathode side) from corrosion. While the binder employed oxidizes in air, it thermally decomposes in nitrogen atmosphere [31]. However, some experiments are conducted only with air. Fig. 7 shows macroscopic structure of the sealing regions obtained at a various N_2 flow rates (100 ml min^{-1}–1000 ml min^{-1}), smaller holes are formed mainly at the middle of sealing region indicating insufficient removal of the burned gas. The shape of holes reveals that the burned gas accumulated at these regions and pushes powders to form holes. At higher flow rates, the number of holes decreases, reducing leakages rate and enhancing the sealing. At 500 ml min^{-1} almost no holes are observed and leakage rate is measured to be less than 0.1 ml min^{-1} which is considered to be an acceptable sealing for the solid oxide fuel cell stack. The flow rate is further increased from 700 ml min^{-1} to 1000 ml min^{-1}. At higher flow rates, small channels are formed which are identified as gas

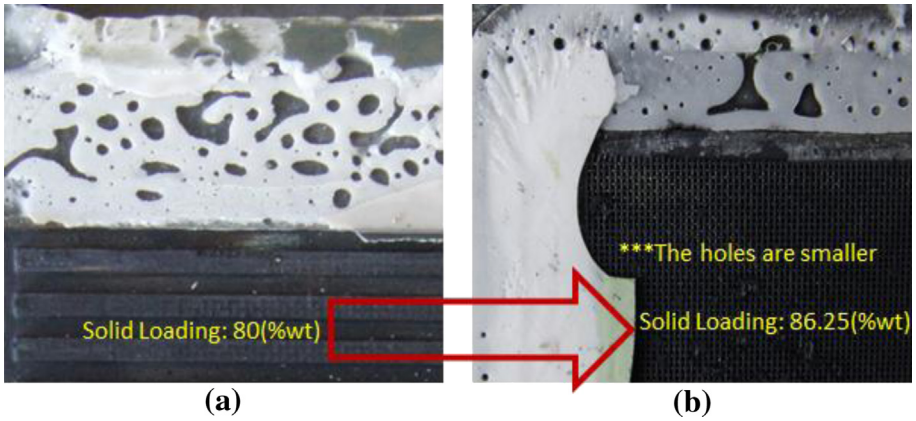

Fig. 6. Effect of Solid loading on the sealing (No-load, No sweep gas and 2 °C min^{-1} + 1 °C min^{-1} heating rate) (a) 80 (%wt) solid loading (b) 86.25 (%wt) solid loading.

Table 2
Effects of solid loading on leakage rates and observations (No-load, No sweep gas and 2 °C min^{-1} + 1 °C min^{-1} heating rate).

Exp.	Solid loading (%wt)	Tape casting result	Sealing qualities	Leakage rates (ml min^{-1})
1	80	✓	x	15.4
2	81.25	✓	x	14.3
3	82	✓	x	12.7
4	82.5	✓	x	12.2
5	85	✓	✓	11.9
6	86.25	✓	✓	10.4
7	87	x	–	–

exhaust path. Size of the channels increases at higher flow rates producing an undesired leak. The same experiments are repeated with air as the sweeping gas. The representative results of the experiments are presented in Fig. 8. Similar sealing structures are observed with those in nitrogen. However, air produces better results at lower flow rates. An allowable leakage is obtained at 200 ml min^{-1} with air instead of 500 ml min^{-1} with that of nitrogen. Almost a hole-free sealing is obtained at 500 ml min^{-1}. All cases considered, the leakage rates and major observations are summarized in Table 3. Table 3 also compares measured leakage results of N_2 and air.

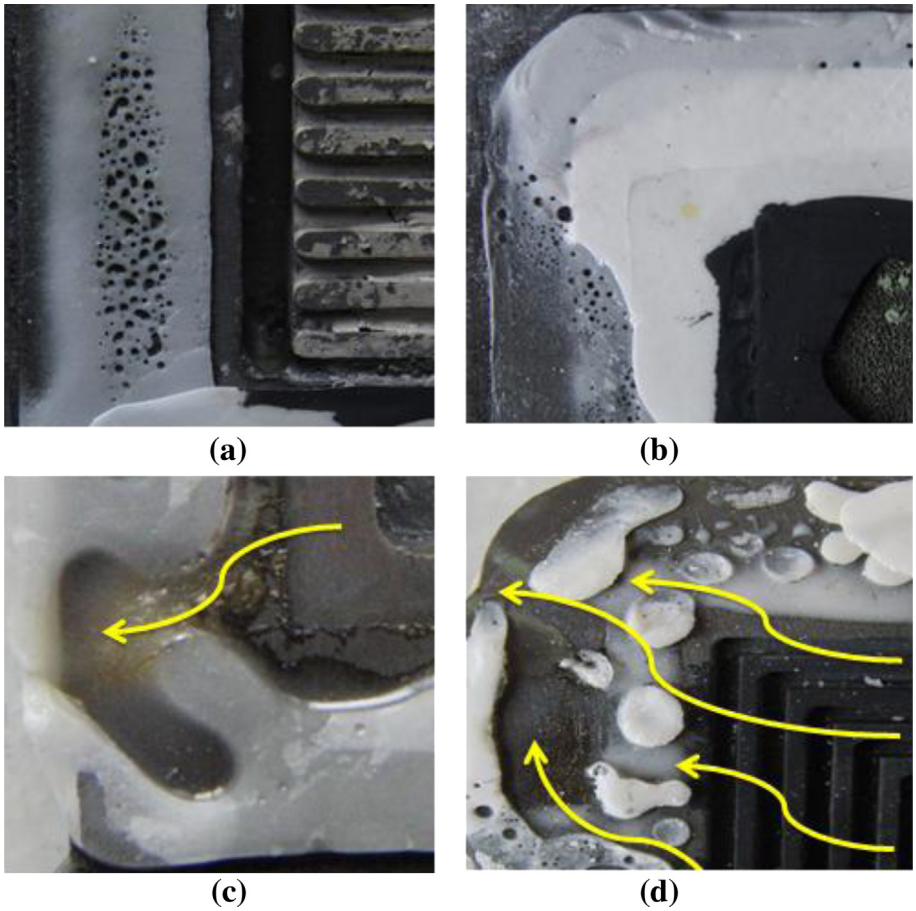

Fig. 7. The effects of sweep gas (N_2) mass flow rates on the sealing (No-load, 2 °C min^{-1} + 1 °C min^{-1}, 86.25 (%wt) solid loading), (a) 200 ml min^{-1}–300 ml min^{-1}, (b) 500 ml min^{-1}, (c) 700 ml min^{-1} (d) 1000 ml min^{-1}.

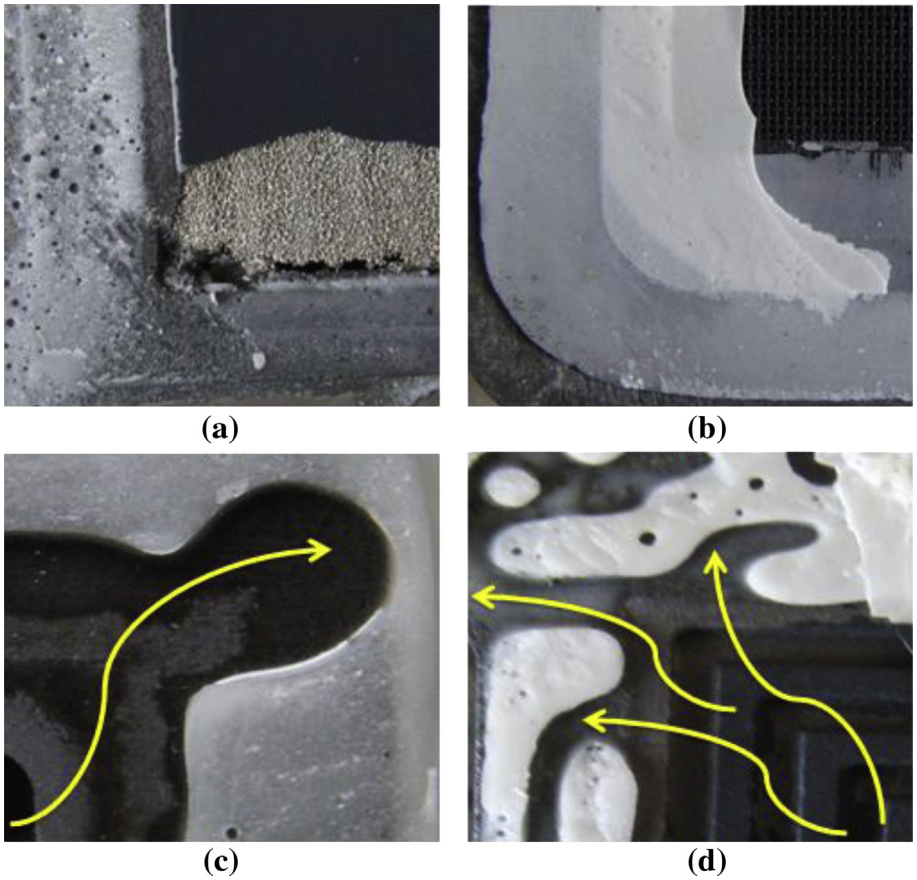

Fig. 8. The effects of sweep gas (air) mass flow rates on the sealing (No-load, 2 °C min^{-1} + 1 °C min^{-1}, 86.25 (%wt) solid loading), (a) 300 ml min^{-1}, (b) 500 ml min^{-1}, (c) 700 ml min^{-1} (d) 1000 ml min^{-1}.

Table 3
The sweep gas effect on the sealing qualities and leakage rates (No-load, 86.25 (%wt) solid loading and 2 °C min^{-1} + 1 °C min^{-1} heating rate).

		N2		*Air*	
Exp.	***Flow Rates (ml·min^{-1})***	***Sealing Qualities***	***Leakage Rates (ml·min^{-1})***	***Sealing Qualities***	***Leakage Rates (ml·min^{-1})***
1	<100	No definite effect	**10.5**	No definite effect	**9.4**
2	200	Better than (1) but not enough	**5.2**	Better than (1) but not enough	**2.5**
3	300	Almost the same with (2)	**3.9**	Very small burn-out holes	**<0.1**
4	500	Holes are smaller than (3)	**<0.1**	No burn-out holes	**<0.1**
5	700	Glass powders are drifted	**18.2**	Glass powders are drifted	**21.1**
6	1000<	Catastrophic glass powders drift	**43.1**	Catastrophic glass powders drift	**45.8**

Table 4
Cases considered for dead weight load and measured leakage rates (500 ml min^{-1} air, 86.25 (%wt) solid loading and 2 °C min^{-1} + 1 °C min^{-1} heating rate).

Exp.	Load (N)	Leakage rates (ml min^{-1})	Burnout qualities
1	No-load	**17.4**	Not enough to keep powders together
2	150	**3.6**	Not enough to keep powders together
3	200	**<0.1**	Optimal load and the best results
4	300	**<0.1**	Burned gas cannot find path for safe removal-individual holes exist
5	400	**<0.1**	Burned gas cannot find path for safe removal-individual holes expand

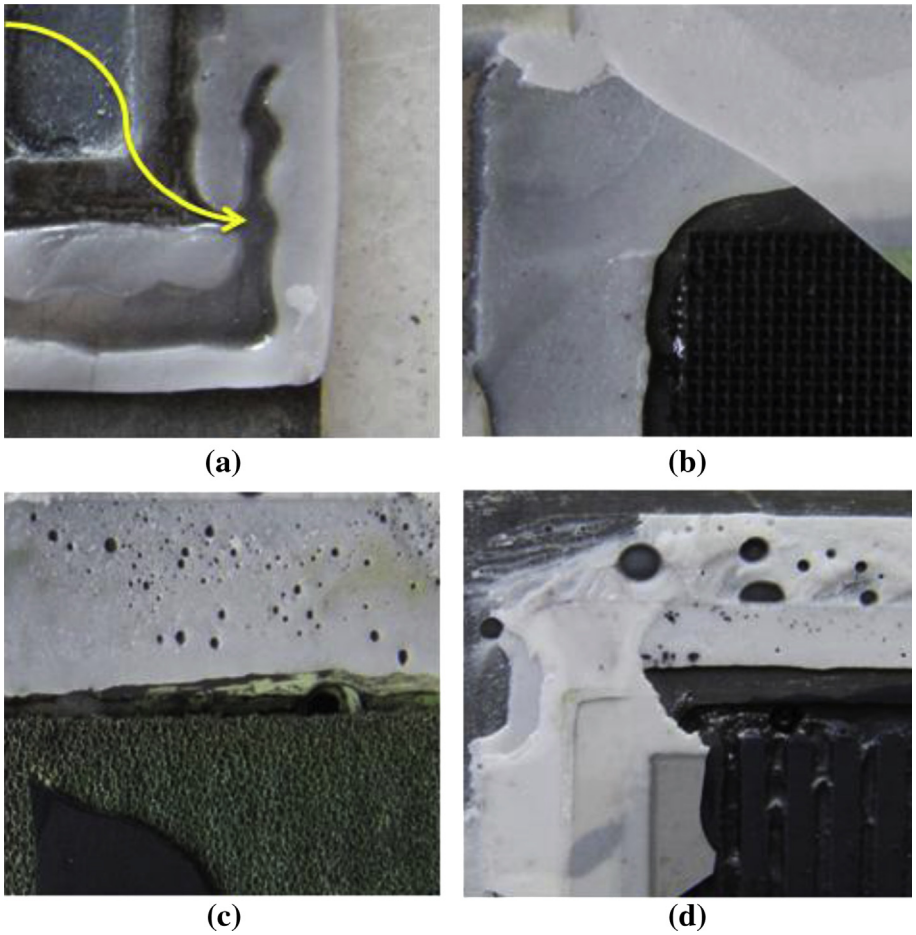

Fig. 9. Effects of dead weight on the sealing (500 ml min^{-1} air, 86.25 (%wt) solid loading and 2 °C min^{-1} + 1 °C min^{-1} heating rate) (a) No-load, (b) 200 N, (c) 300 N, (d) 400 N.

3.4. Effects of dead weight load

A better sealing is usually obtained with a load applied on the cell during the sintering processes. A set of experiments is conducted to optimize the load on the cell during the sealing process. The cases considered are summarized in Table 4. The load is change from 0 to 400 N. Since an adequate sealing is obtained after 200 N, experiments are terminated after 400 N. It is found that even a small load significantly improve the sealing. After a 200 N load leakage rate drops 0.1 ml min^{-1} which can be hardly detectable with the measuring setup and considered to be appropriate for SOFC. The morphology of the sealing depending on the dead weight is illustrated in Fig. 9. It is seen that when no-load is applied, sweeping gas forms a path to leave the sealing region. However when a load of 200 N is applied, the particles cannot leave their position during the binder burnout and provide very good sealing. Fig. 9c and d suggests that too much pressure has an adverse effect on the gas to escape. Some of gas are trapped between the particles and increase the local pressure creating subsequent hole in the sealing. Larger holes are observed at higher pressures suggest that higher loads do not allow some of the burned gases to leave easily from the sealing area. Therefore, a 200 N load is considered to be optimal for a better sealing.

4. Conclusions

The sealing between ceramic electrolyte and metallic interconnector of an SOFC stack with a glass–ceramic sealant is investigated in a wide parameter range. Effect of heating rate, solid loading, sweep gas type and their flow rate and load on the cells are considered. A slow heating schedule is usually required to remove the binders and sintering of glass ceramic powders while chemically bonding electrolyte and interconnector materials. The carrier gas type is found to be critically important for removing organic binders. While an inert gas (N_2, Ar) prevents the metallic interconnector from oxidation at the anode side during the binder burnout process, they are not enough to remove all binders. Therefore, air flow is found to improve burning of binders. A low sweeping air flow rate is found to be insufficient to remove the burned gas, however too high air flow deteriorates the sealing performance by removing some of the powders before sintering. It is shown that higher solid loading enhances the sealing performance, however the highest solid loading is found to be limited with manufacturing method. Since the tape casting method is employed in this study, a maximum 86.25% solid loading is achieved. The load on the cell (dead weight) is optimized to balance keeping glass powders stable and providing a safe removal path for the burned gas.

References

[1] D. Gödeke, J. Besinger, Y. Pflügler, B. Reuedinger, ECS Trans. 25 (2009) 1483–1490.
[2] D. Gödeke, U. Dahlmann, J. Power Sources 196 (2011) 9046–9050.
[3] Y.S. Chou, E.C. Thomsen, J.P. Choi, J.W. Stevenson, J. Power Sources 197 (2012) 154–160.
[4] Y.S. Chou, E.C. Thomsen, R.T. Williams, J.P. Choi, N.L. Canfield, J.F. Bonnett, J.W. Stevenson, A. Shyam, E.L. Curzio, J. Power Sources 196 (2011) 2709–2716.

[5] K.D. Meinhardt, D.S. Kim, Y.S. Chou, K.S. Weil, J. Power Sources 182 (2008) 188–196.
[6] S.M. Gross, D. Federmann, J. Remmel, M. Pap, J. Power Sources 196 (2011) 7338–7342.
[7] F. Smeacetto, M. Salvo, M. Santarelli, P. Leone, G.A. Ortigoza-Villalba, A. Lanzini, L.C. Ajitdoss, M. Ferraris, Int. J. Hydrogen Energy 38 (2013) 588–596.
[8] L. Blum, S.M. Groß, J. Malzbender, U. Pabst, M. Peksen, R. Peters, I.C. Vinke, J. Power Sources 196 (2011) 7175–7181.
[9] C.B. Carter, M.G. Norton, Ceramic Materials Science and Engineering, Springer, 2007.
[10] P. Singh, N.P. Bansal, Advances in Solid Oxide Fuel cells IV, Wiley, Florida, 2008.
[11] T.A. Ring, Fundamentals of Ceramic Powder Processing and Synthesis, Academic Press, 1996.
[12] S.C. Singhal, K. Kendall, High temperature Solid Oxide Fuel Cells Fundamentals, Design and Application, Elsevier, 2003.
[13] J.S. Reed, Principles of Ceramic Processing, John Wiley and Sons, Inc., 1995.
[14] R. Mauczok, V.T. Zaspalis, J. Eur. Ceram. Soc. 20 (2000) 2121–2127.
[15] F.A. Cetinel, W. Bauer, R. Knitter, J. Haußelt, Ceram. Int. 37 (2011) 2809–2820.
[16] E.S. Thian, N.H. Loh, K.A. Khor, S.B. Tor, Adv. Powder Technol. 12 (2001) 361–370.
[17] M. Salehi, F. Clemens, T. Graule, B. Grobéty, Appl. Energy 95 (2012) 147–155.
[18] L.C.K. Liau, C.C. Chen, J. Power Sources 177 (2008) 1–8.
[19] B.J. Cho, E.T. Park, J.M. Lee, J. Eur. Ceram. Soc. 29 (2009) 451–456.
[20] Y. Saito, J. Nyumura, Y. Zhang, S. Tanaka, N. Uchida, K. Uematsu, J. Eur. Ceram. Soc. 22 (2002) 2835–2840.
[21] Z. Shi, Z.X. Guo, Mater. Sci. Eng. A 365 (2004) 129–135.
[22] Y. Shengjie, Y.C. Lam, J.C. Chai, K.C. Tam, Comput. Mater. Sci. 30 (2004) 496–503.
[23] V.A. Krauss, A.A.M. Oliveira, A.N. Klein, H.A. Al-Qureshi, M.C. Fredel, J. Mater. Process. Technol. 182 (2007) 268–273.
[24] R.K. Enneti, T.S. Shivashankar, S.J. Park, R.M. German, S.V. Atre, Powder Technol. 228 (2012) 14–17.
[25] W. Liu, X. Yang, Z. Xie, C. Jia, L. Wang, J. Eur. Ceram. Soc. 32 (2012) 2187–2191.
[26] V.P. Onbattuvelli, R.K. Enneti, S.J. Park, S.V. Atre, Int. J. Refract. Met. Hard Mater. 36 (2013) 77–84.
[27] http://www.ceradyneviox.com/products/products.aspx?MarketID=14, 15.04.2013.
[28] Y. Palaci, B. Timurkutluk, Int. J. Energy Res. (2012), http://dx.doi.org/10.1002/er.2958.
[29] B. Timurkutluk, S. Celik, C. Timurkutluk, M.D. Mat, Y. Kaplan, Int. J. Hydrogen Energy 37 (2012) 13499–13509.
[30] B. Timurkutluk, S. Celik, S. Toros, C. Timurkutluk, M.D. Mat, Y. Kaplan, Ceram. Int. 38 (2012) 5651–5659.
[31] http://www.butvar.com/pdfs/en/Updated_Butvar_Ceramic_Binder_Bulletin_V5.pdf, 15.04.2013.